Droplet epitaxy quantum dots based infrared photodetectors

Droplet epitaxy quantum dots for infrared photodetectors

Stefano Vichi,[1] Sergio Bietti,[1] Arastoo Khalili,[2] Matteo Costanzo,[1] Federica Cappelluti,[2] Luca Esposito,[1] Claudio Somaschini,[3] Alexey Fedorov,[4] Shiro Tsukamoto,[1] Patrick Rauter,[5] and Stefano Sanguinetti[1]

[1)] *LNESS and Department of Materials Science, University of Milano-Bicocca, via Cozzi 55, 20125 Milano, Italy*

[2)] *Department of Electronics and Telecommunications, Politecnico di Torino, Corso Duca degli Abruzzi 24, 10129 Torino, Italy*

[3)] *PoliFab - Politecnico di Milano, via Colombo 81, 20133 Milano, Italy*

[4)] *CNR–IFN and LNESS, via Anzani 42, 22100 Como, Italy*

[5)] *Institute of Semiconductor and Solid State Physics, Johannes Kepler University of Linz, Altenberger Strae 69, 4040 Linz, Austria*

I. ABSTRACT

The fabrication and characterization of an infrared photodetector based on GaAs droplet epitaxy quantum dots embedded in $Al_{0.3}Ga_{0.7}As$ barrier is reported. The high control over dot electronic properties and the high achievable number density allowed by droplet epitaxy technique permitted us to realize a device using a single dot layer in the active region. Moreover, thanks to the independent control over dot height and width, we were able to obtain a very sharp absorption peak in the thermal infrared region (3-8 μm). Low temperature photocurrent spectrum was measured by Fourier spectroscopy, showing a narrow peak at 198 meV ($\sim$ 6.3 μm) with a full width at half maximum of 25 meV. The observed absorption is in agreement with theoretical prediction based on effective mass approximation of the dot electronic transition.

II. INTRODUCTION

In recent years the market of infrared (IR) devices is continuously growing, pushed by the great number of applications in commercial, public and academic domains. However, the further development of IR sensors for imaging purposes is closely linked to the development of a new generation of sensor: the "third generation"[1].

This new generation should provide photodetectors with enhanced capabilities such as larger number of pixels, higher frame rates, better thermal resolution and multispectral functionality. In the IR region four major photodetector technologies are developing multispectral capabilities: the HgCdTe photodiodes, the quantum well (QWIP) and quantum dot (QDIP) infrared photodetectors and antimonide based type II superlattice photodiodes[2,3]. The last three technologies are based on quantum heterostructures, making them suitable for easy integration in present technology. Monolithic silicon integration of both As and Sb materials, at the basis of the three technologies, have been already demonstrated[4–6]. Between these, bulk HgCdTe is at present times the most advanced technology, with better overall performances and a wide and tunable detection window[7]. However, QDIP photodetectors are emerging as a promising technology, due to the high control over transition energies originating from 3D carrier confinement and the absence of limiting selection rules, which hinder the widespread use of QWIP technology[7,8]. The active part of these detectors consists

of multiple layers of self-assembled quantum dots (QDs) embedded in a barrier layer with a larger band gap for carrier confinement in three dimensions. QDs are usually self-assembled via the Stranski-Krastanov (SK) growth mode, which exploits the strain induced by lattice mismatch between substrate and epilayer to assemble the nanostructures[9–11]. However, there are several drawbacks which need to be overcome before SK-QD based QDIPs may become the leading technology in the thermal infrared (TIR) range. The main disadvantage of SK-QDIPs is related to the large size dispersion which broadens the absorption spectrum and subsequently lowers quantum efficiency[12]. The other drawbacks, related to the growth process, are the presence of strain-related defects and of a wetting layer which lowers the carrier confining barrier. Most of these shortcomings can be overcome by using droplet epitaxy (DE), an alternative technique to grow self-assembled QDs in lattice-matched materials[13–18]. The DE is a flexible growth method performed in MBE environment, which allows for the fabrication of three-dimensional nanostructures with different geometries, such as quantum dots, quantum molecules, concentric multiple quantum rings and many others[19–23]. In the case of GaAs growth by DE, the substrate is first irradiated by a Ga beam, leading to the formation of nanometer-size Ga droplets with uniform size. The droplets are subsequently crystallized into GaAs nanostructures by an As_4 beam supply. The first step allows for a precise control on the final density and size of the nanostructures[24], the second step, controlling the Ga diffusion on the surface, allows for the formation of nanostructures with different shapes and electronic properties[25–27]. The much higher control over the dot nucleation process allows to tune independently QD geometry, width, thickness and density and to achieve a lower size dispersion[28], which leads to a higher absorption coefficient and a narrower bandwidth. These advantages make DE a very interesting technique to grow quantum dots, in particular for photodetectors where high absorption coefficient and narrow bandwidth are required. In this paper we present the first example of working QDIP for TIR detection based on a single layer of high density GaAs/$Al_{0.3}Ga_{0.7}As$ DE-QDs.

III. EXPERIMENTAL PROCEDURE

The growth was performed in a molecular beam epitaxy (MBE) system, starting from an intrinsic double polished 2" GaAs(001) just substrate. The structure consists of an active region sandwiched between two contact layers. The bottom contact consists of a layer of

1.5 μm Si-doped GaAs layer with a nominal doping of $2 \cdot 10^{18}$ cm^{-3}, followed by 100 nm of Si-doped $Al_{0.3}Ga_{0.7}As$ with a nominal doping of $3 \cdot 10^{17}$ cm^{-3}. The active region is made of 700 nm thick intrinsic $Al_{0.3}Ga_{0.7}As$ layer in which, at the center, a single GaAs QDs layer is embedded. The QDs, grown by droplet epitaxy, are filled by an underlying δ-doping layer positioned 3 nm apart from the QDs, providing nominally 6 electrons per dot. QD growth conditions were optimized to obtain the desired size and density by growing a series of uncapped samples and characterizing them by atomic force microscopy (AFM), performed in tapping mode and using a tip with a lateral resolution of 2 nm. Following the intrinsic region, 100 nm of Si-doped $Al_{0.3}Ga_{0.7}As$ with a doping of $3 \cdot 10^{17}$ cm^{-3} were grown. Finally, 1 μm of n doped GaAs with a doping density of $2 \cdot 10^{18}$ cm^{-3} was deposited as a top contact.

More in details, the growth rate was kept at 0.5 ML/s for the GaAs and 0.71 ML/s for the AlGaAs layers, the substrate temperature was set to 580°C and 650°C for GaAs and AlGaAs, respectively. QDs were grown by depositing 3ML of Ga at a rate of 0.1 ML/s with a substrate temperature of 180°C. At the same temperature the crystallization was performed by supplying As at a beam equivalent pressure of $5 \cdot 10^{-5}$ Torr. After the growth, standard photolithography was used for structuring the device. Mesa etching was done by a wet approach, using an H_3PO_4:H_2O_2:H_2O solution with 1:2.5:8 relative concentrations. Metal contacts were finally deposited by e-beam evaporation using a stack of Ge(26 nm)/Au(54 nm)/Ni(15 nm) and annealed at 420°C for 5 s in Ar forming gas, in order to get ohmic contacts as confirmed by I-V measurements. The device structure is shown in figure 1.

For optoelectronic characterization at cryogenic temperatures, the devices were contacted by wire bonding and mounted in a cryostat.

IV. RESULTS AND DISCUSSION

The quantum dot geometry was studied by atomic force microscopy (AFM) on an uncapped sample. As can be seen from the inset of figure 2a, the shape of the dots shows a slight asymmetry due to the diffusion coefficient of Ga adatoms being larger along $<1\bar{1}0>$ compared to <110> direction[29].

We defined the width of the dots as the diameter of the circle which gives the same projected area as the dot. Accordingly, from the analysis of the AFM images (figure 2a) we calculated a dot density of $4{\cdot}10^{10}$ cm^{-2} with a mean height of (5.1 ± 1) nm and a diameter

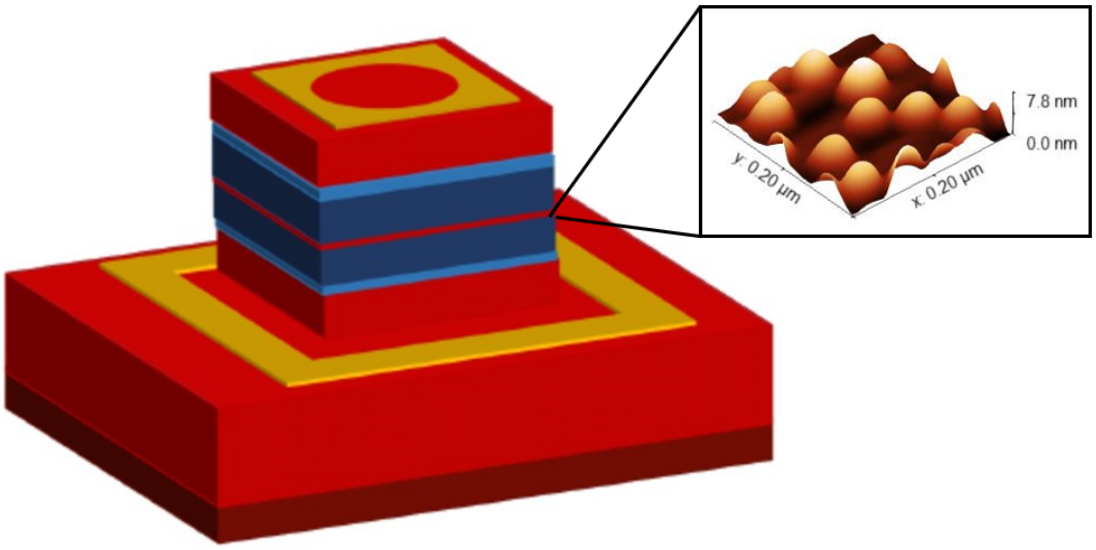

FIG. 1: Design of the device, where different materials are represented by different colors: gold for the contacts, red for GaAs, light blue for doped $Al_{0.3}Ga_{0.7}As$ and blue for intrinsic $Al_{0.3}Ga_{0.7}As$. The size of the mesa is 1x1 μm^2. The inset shows a 200x200 nm^2 AFM scan of the QDs.

of (36 ± 8) nm. The height distribution of QDs is shown in the histogram of figure 2b.

In order to calculate QD transition energy and broadening from the measured dot dimensions, we have implemented a simulation code based on effective mass approximation in cylindrical coordinates[30]. For this purpose, we modeled the dots as truncated cones[25], with height and width as obtained from the AFM analysis. From the simulations, we obtained an intersubband absorption peak at 183 meV involving ground state and the last excited state of QD with a FWHM of 20 meV.

Figure 3 shows the energy band diagram at thermal equilibrium and room temperature of the QDIP under study. We calculated the device band diagram using a quantum-corrected transport-Poisson model[31,32]. Material parameters are taken from the literature assuming $GaAs/Al_{0.3}Ga_{0.7}As$ CB discontinuity of 62%, as determined by C-V profiling technique[33]. The device exhibits two sharp band discontinuities due to the presence of the doped AlGaAs

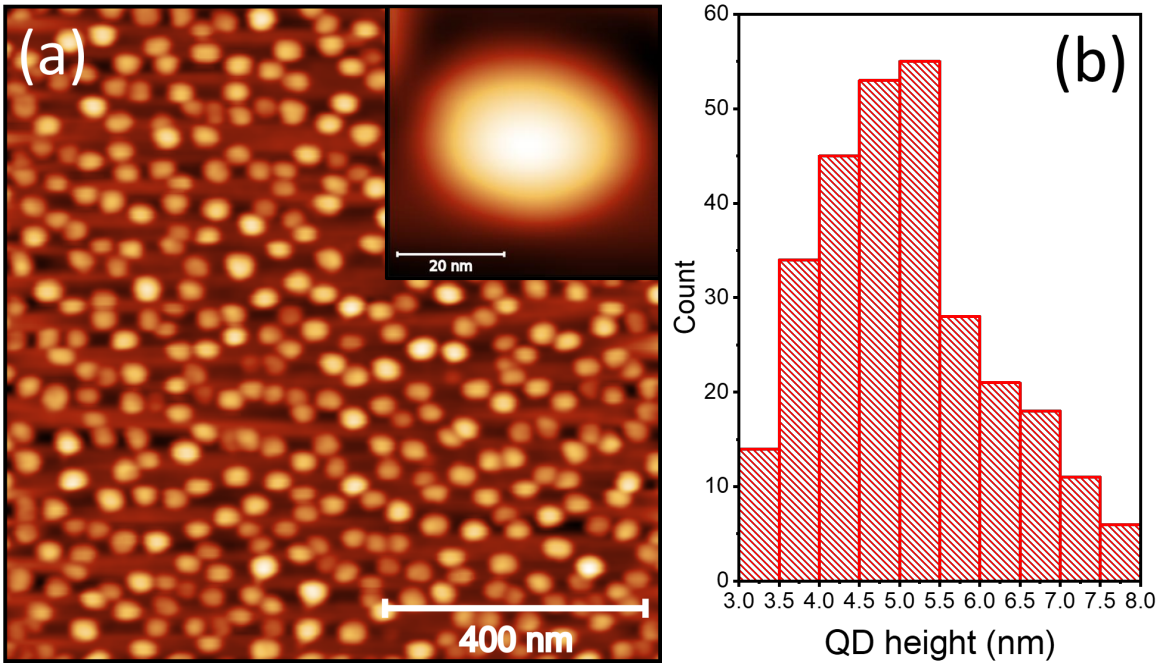

FIG. 2: (a) AFM image of the dot population of the uncapped sample. The dot density is $4{\cdot}10^{10}$ cm^{-2} with a height of (5.1 ± 1) nm and a diameter of (36 ± 8) nm. The inset shows the AFM image of a quantum dot. (b) Height histogram of the QDs of panel a.

regions which could enhance carrier injection into the semi-insulating material.

The optoelectronic characterization of the devices was performed at a temperature of 77 K by applying a bias to the top contact with respect to the bottom one and measuring the resulting current. Figure 4 shows typical dark-current characteristics, obtained by blocking the cryostat windows by a cooled shield. The asymmetry of the dark-current curve is most likely related to an asymmetric charge distribution along the growth direction. The latter is probably due to the large band offset between the GaAs and AlGaAs regions in combination with the low operating temperature.

Photocurrent spectra were obtained in lock-in technique by illuminating the device by the chopped globar source in a Fourier-transform infrared spectrometer (FTIR). The QDIP current response was measured by a low-noise current amplifier and employed as FTIR detector input. Figure 5 shows the photocurrent spectrum recorded at an applied bias of -2 V, featuring a narrow peak with a full width of half maximum of 25 meV centered around 198 meV. This result is in good agreement with the simulated dot transition energy at 183 meV (dashed lines in figure 5) with a FWHM of 20 meV, clearly indicating that the

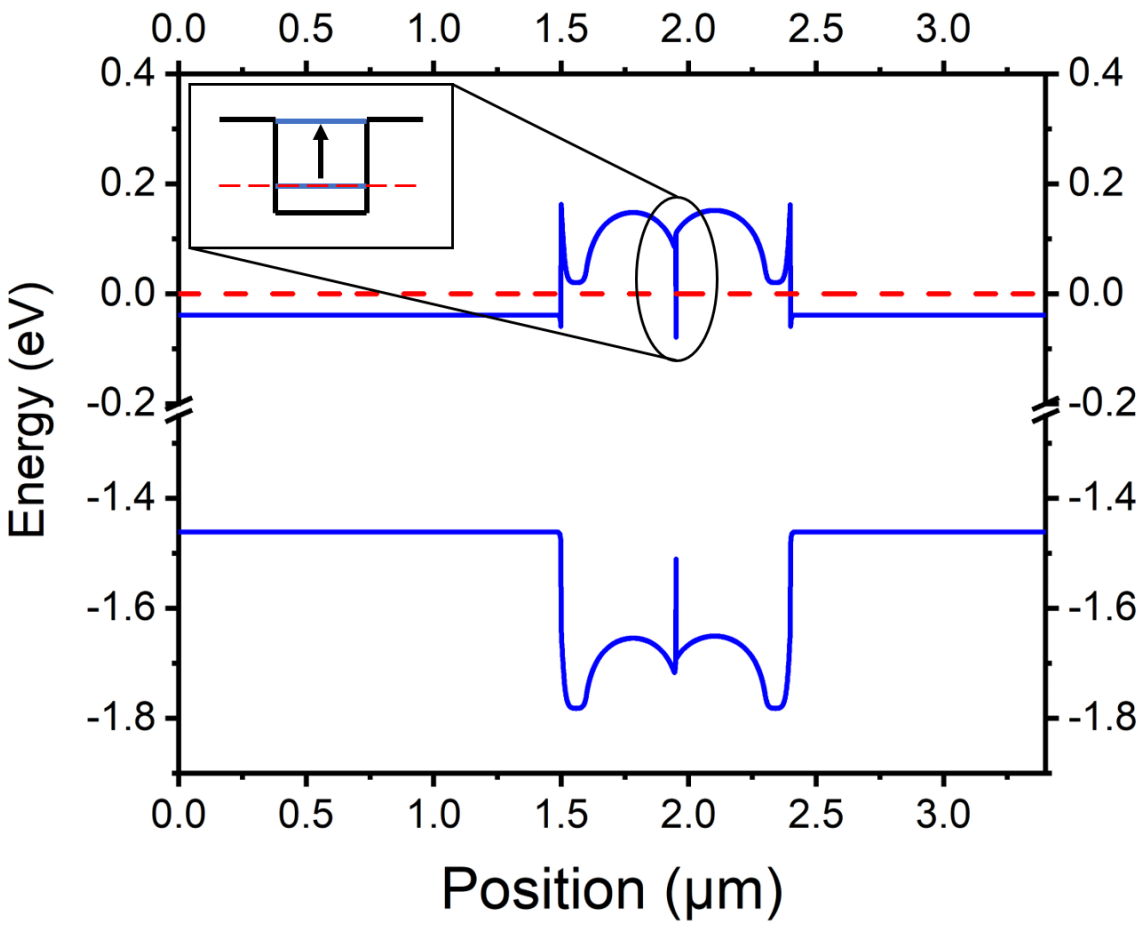

FIG. 3: Structure of the device and band alignment of the QDIP under study. The inset shows the calculated QDs ground and excited state involved in the transition.

photocurrent peak originates from a quantum dot intersubband transition. The very narrow absorption linewidth (12% of peak wavelength) is comparable to confined transitions in QWIP[34], where size dispersion is negligible. A similarly narrow linewidth was also observed in InAs/GaAs QDs[11], demonstrating that extremely sharp intersubband transitions can be obtained even with QDs height fluctuation of 20%. The agreement between calculated absorption spectrum, based on QD shapes measured by AFM scanning of uncapped samples, and the observed one calls for a flexible and controllable engineering of the droplet epitaxy process together with a limited interdiffusion at the QD interfaces which maintains the actual QD size during the capping process[14].

The high degree of control on the QD electronic properties obtained via droplet epitaxy permits an unprecedented engineering of the QDIP active layer and show its potential for

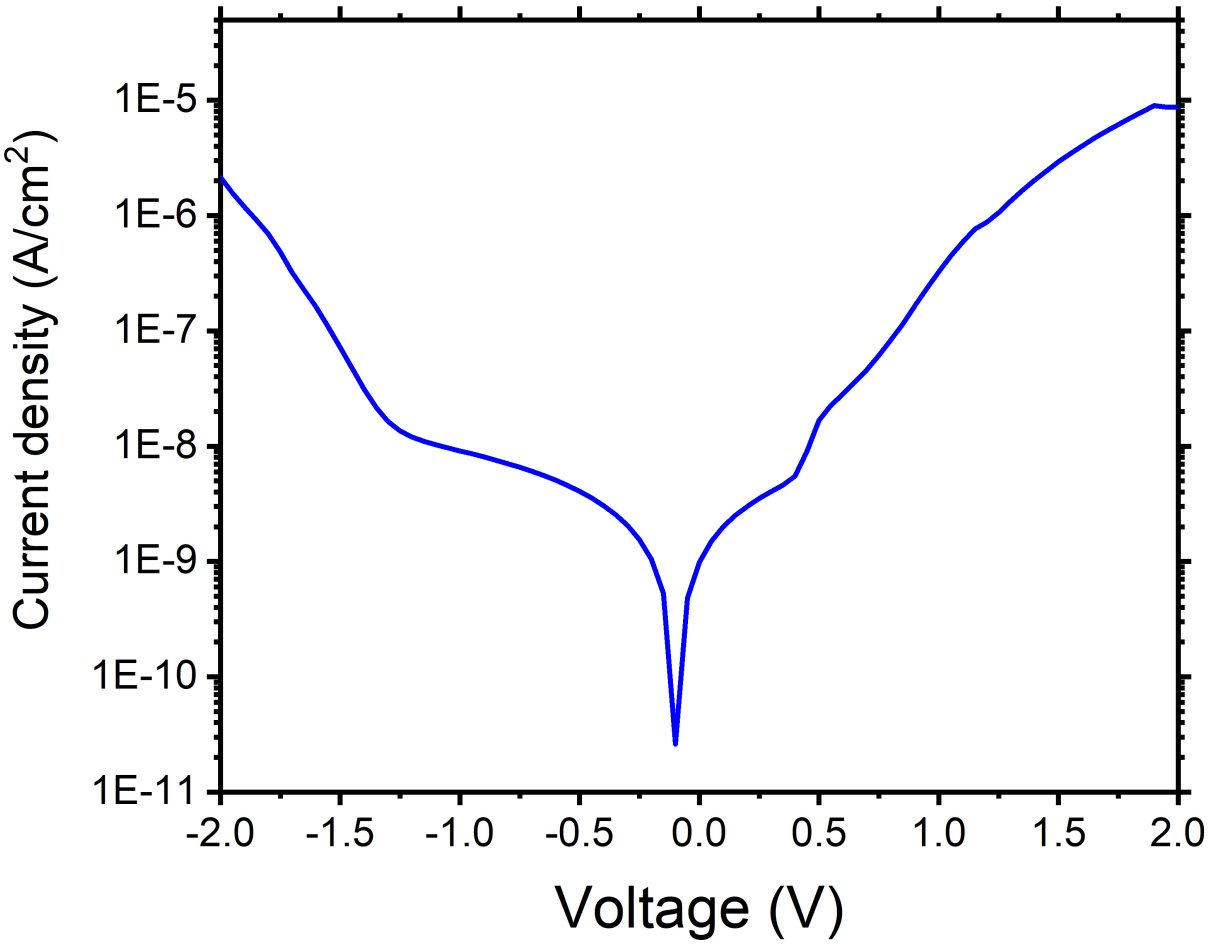

FIG. 4: Dark current density measured at 77 K from -2 V to +2 V.

applications where an optical intersubband transition with a precisely selectable energy and a narrow linewidth is required. On top of that, we demonstrated that is possible to obtain a detectable photocurrent signal with only a single layer of quantum dots, a possibility offered by droplet epitaxy only, due to the high areal density of QDs ($4{\cdot}10^{10}$ cm^{-2}) and the reduction of the thermionic escape of carriers due to the removal of the wetting layer at the base of the QDs[35].

Since the absorption spectrum is strictly related to QDs geometrical properties, we can estimate its reproducibility by considering all the possible sources of error during the growth process. More into details, we can safely assume a total error of half second in the electronic control of the opening/closing sequence of the Ga shutter during droplet formation and a fluctuation of $\pm$ 2.5°C in substrate temperature. The first error gives a fluctuation of 0.05 MLs in the amount of deposited Ga which, by simple geometrical calculations, results in

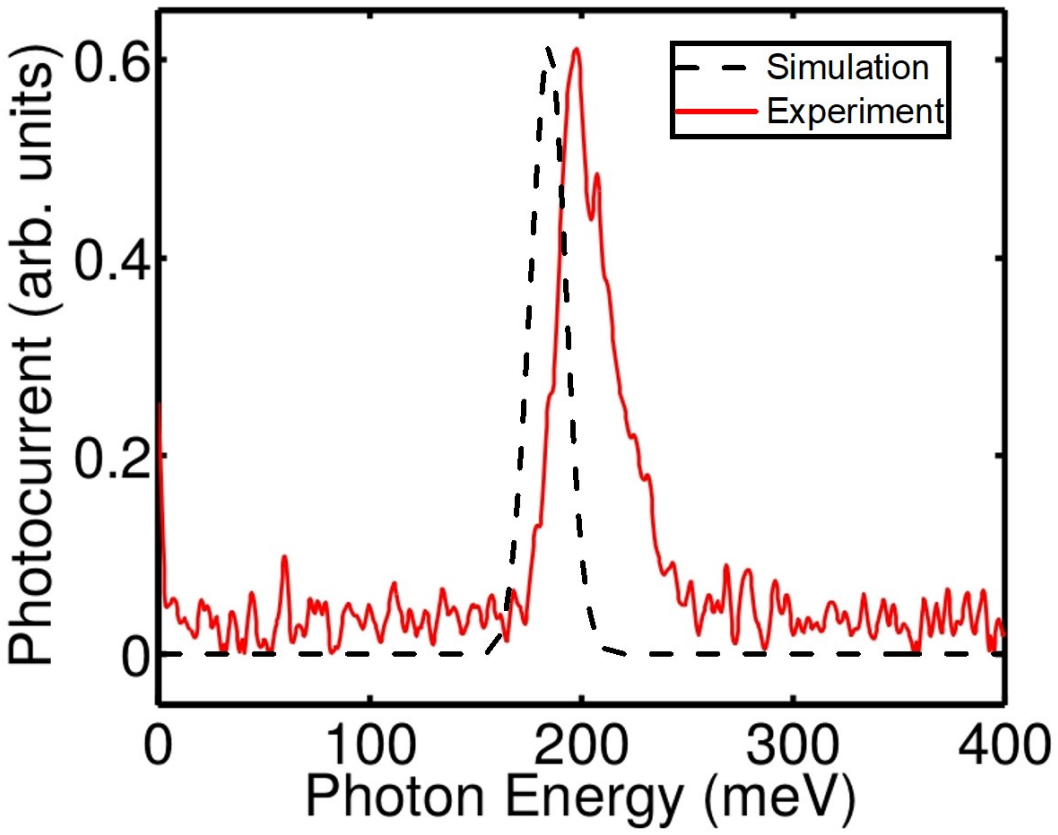

FIG. 5: Photocurrent spectrum measured at 77 K and a bias of -2 V (red line). The dashed line shows the simulated transition considering the height dispersion.

a height difference of less than 1 angstrom. Temperature fluctuations instead affects QDs density as predicted by the standard nucleation theory[36] and reported in literature[24,37]. The maximum estimated temperature oscillation of (180±2.5)°C can change the measured QD mean height from 4.9 nm (at 177.5°C) to 5.3 nm (at 182.5°C), which lies within the FWHM of the measured height distribution. Therefore we can conclude that experimental deviations from the optimal growth conditions of the high-density QD layer does not affect significantly the absorption spectrum.

These results can open interesting perspectives for DE-based QDIP, in terms of precise wavelength control and extremely high density of nanostructures.

V. CONCLUSIONS

The higher number of independent parameters (QD geometry, dimensions and density) and the narrow size dispersion make DE-QDIP a promising alternative to SK-QDIP for IR detection, in particular when a narrow absorption band is required[38]. In this work, we report the first example of a working QDIP based on a single layer of high-density DE-QDs, suitable for TIR detection. The high dot density achieved allowed us to observe a clear photocurrent signal for a single layer of QDs. The high uniformity of DE-QDs resulted in a photocurrent peak centered at 198 meV with a narrow bandwidth of 25 meV. The identification of the measured peak with a QD transition was confirmed by simulations based on effective mass approximation. We believe that the ability to finely tune the geometrical properties of QDs makes droplet epitaxy an attractive technique for QDIPs, since it can overcome most of the limiting problems of the current generation of quantum dot-based detectors.

VI. ACKNOWLEDGEMENT

The authors acknowledge financial support through Italian Space Agency (ASI) project Silicio Rosso.

REFERENCES

[1]A. Rogalski, J. Antoszewski, and L. Faraone, "Third-generation infrared photodetector arrays," Journal of Applied Physics **105** (2009).

[2]C. Downs and T. E. Vandervelde, "Progress in infrared photodetectors since 2000," Sensors (Switzerland) **13**, 5054–5098 (2013).

[3]C. L. Tan and H. Mohseni, "Emerging technologies for high performance infrared detectors," Nanophotonics **7**, 169–197 (2018).

[4]S. Bietti, A. Scaccabarozzi, C. Frigeri, M. Bollani, E. Bonera, C. V. Falub, H. Von Känel, L. Miglio, and S. Sanguinetti, "Monolithic integration of optical grade GaAs on Si (001) substrates deeply patterned at a micron scale," Applied Physics Letters **103** (2013), 10.1063/1.4857835.

[5]L. Cavigli, S. Bietti, N. Accanto, S. Minari, M. Abbarchi, G. Isella, C. Frigeri, A. Vinattieri, M. Gurioli, and S. Sanguinetti, "High temperature single photon emitter monolithically integrated on silicon," Applied Physics Letters **100** (2012), 10.1063/1.4726189.

[6]O. P. Bolkhovityanov, Yu B and Pchelyakov, "GaAs epitaxy on Si substrates: modern status of research and engineering," Uspekhi Fizicheskih Nauk **178**, 459 (2008).

[7]A. Rogalski, "Infrared detectors: An overview," Infrared Physics and Technology **43**, 187–210 (2002).

[8]P. Martyniuk and A. Rogalski, "Quantum-dot infrared photodetectors: Status and outlook," Progress in Quantum Electronics **32**, 89–120 (2008).

[9]S. Raghavan, P. Rotella, A. Stintz, B. Fuchs, S. Krishna, C. Morath, D. A. Cardimona, and S. W. Kennerly, "High-responsivity, normal-incidence long-wave infrared (λ=7. 2μm) InAs/In0.15Ga0.85As dots-in-a-well detector," Applied Physics Letters **81**, 1369–1371 (2002).

[10]S. F. Tang, S. Y. Lin, and S. C. Lee, "Near-room-temperature operation of an InAs/GaAs quantum-dot infrared photodetector," Applied Physics Letters **78**, 2428–2430 (2001).

[11]Z. Chen, O. Baklenov, E. T. Kim, I. Mukhametzhanov, J. Tie, A. Madhukar, Z. Ye, and J. C. Campbell, "Normal incidence InAs/AlxGa1-xAs quantum dot infrared photodetectors with undoped active region," Journal of Applied Physics **89**, 4558–4563 (2001).

[12]J. Phillips, "Evaluation of the fundamental properties of quantum dot infrared detectors," Journal of Applied Physics **91**, 4590–4594 (2002).

[13]K. Watanabe, N. Koguchi, and Y. Gotoh, "Fabrication of GaAs Quantum Dots by Modified Droplet Epitaxy," Japanese Journal of Applied Physics **39**, 79–81 (2000).

[14]J. G. Keizer, J. Bocquel, P. M. Koenraad, T. Mano, T. Noda, and K. Sakoda, "Atomic scale analysis of self assembled GaAs/AlGaAs quantum dots grown by droplet epitaxy," Applied Physics Letters **96**, 062101 (2010).

[15]M. Gurioli, Z. Wang, A. Rastelli, T. Kuroda, and S. Sanguinetti, "Droplet epitaxy of semiconductor nanostructures for quantum photonic devices," Nature Materials **18**, 799–810 (2019).

[16]V. Mantovani, S. Sanguinetti, M. Guzzi, E. Grilli, M. Gurioli, K. Watanabe, and N. Koguchi, "Low density GaAs/AlGaAs quantum dots grown by modified droplet epitaxy," Journal of Applied Physics **96**, 4416–4420 (2004).

[17]K. Reyes, P. Smereka, D. Nothern, J. M. Millunchick, S. Bietti, C. Somaschini, S. Sanguinetti, and C. Frigeri, "Unified model of droplet epitaxy for compound semiconductor nanostructures: Experiments and theory," Physical Review B - Condensed Matter and Materials Physics **87**, 1–14 (2013), arXiv:1211.0486.

[18]F. Basso Basset, S. Bietti, M. Reindl, L. Esposito, A. Fedorov, D. Huber, A. Rastelli, E. Bonera, R. Trotta, and S. Sanguinetti, "High-Yield Fabrication of Entangled Photon Emitters for Hybrid Quantum Networking Using High-Temperature Droplet Epitaxy," Nano Letters **18**, 505–512 (2018), arXiv:1710.03483.

[19]J. Wu, Z. Li, D. Shao, M. O. Manasreh, V. P. Kunets, Z. M. Wang, G. J. Salamo, and B. D. Weaver, "Multicolor photodetector based on GaAs quantum rings grown by droplet epitaxy," Applied Physics Letters **94**, 3–5 (2009).

[20]J. Wu, D. Shao, V. G. Dorogan, A. Z. Li, S. Li, E. a. DeCuir, M. O. Manasreh, Z. M. Wang, Y. I. Mazur, and G. J. Salamo, "Intersublevel infrared photodetector with strain-free GaAs quantum dot pairs grown by high-temperature droplet epitaxy." Nano letters **10**, 1512–6 (2010).

[21]T. Mano, T. Kuroda, S. Sanguinetti, T. Ochiai, T. Tateno, J. Kim, T. Noda, M. Kawabe, K. Sakoda, G. Kido, and N. Koguchi, "Self-assembly of concentric quantum double rings," Nano Letters **5**, 425–428 (2005).

[22]C. Somaschini, S. Bietti, N. Koguchi, and S. Sanguinetti, "Fabrication of multiple concentric nanoring structures," Nano Letters **9**, 3419–3424 (2009).

[23]C. Somaschini, S. Bietti, N. Koguchi, and S. Sanguinetti, "Shape control via surface reconstruction kinetics of droplet epitaxy nanostructures," Applied Physics Letters **97**, 1–4 (2010).

[24]C. Heyn, A. Stemmann, A. Schramm, H. Welsch, W. Hansen, and Á. Nemcsics, "Regimes of GaAs quantum dot self-assembly by droplet epitaxy," Physical Review B - Condensed Matter and Materials Physics **76**, 1–4 (2007).

[25]S. Bietti, J. Bocquel, S. Adorno, T. Mano, J. G. Keizer, P. M. Koenraad, and S. Sanguinetti, "Precise shape engineering of epitaxial quantum dots by growth kinetics," Physical Review B **92**, 075425 (2015).

[26]S. Bietti, C. Somaschini, and S. Sanguinetti, "Crystallization kinetics of Ga metallic nanodroplets under As flux," Nanotechnology **24** (2013), 10.1088/0957-4484/24/20/205603.

[27]S. Bietti, C. Somaschini, S. Sanguinetti, N. Koguchi, G. Isella, and D. Chrastina, "Fabrication of high efficiency III-V quantum nanostructures at low thermal budget on Si," Applied Physics Letters **95** (2009), 10.1063/1.3273860.

[28]F. B. Basset, S. Bietti, A. Tuktamyshev, S. Vichi, E. Bonera, and S. Sanguinetti, "Spectral broadening in self-assembled GaAs quantum dots with narrow size distribution," J. Appl. Phys. **126**, 024301 (2019).

[29]C. Somaschini, S. Bietti, A. Fedorov, N. Koguchi, and S. Sanguinetti, "Concentric Multiple Rings by Droplet Epitaxy: Fabrication and Study of the Morphological Anisotropy," Nanoscale Research Letters **5**, 1865–1867 (2010).

[30]J. Y. Marzin and G. Bastard, "Calculation of the energy levels in quantum dots," Solid State Communications **92**, 437–442 (1994).

[31]M. Gioannini, A. P. Cedola, N. Di Santo, F. Bertazzi, and F. Cappelluti, "Simulation of quantum dot solar cells including carrier intersubband dynamics and transport," IEEE Journal of Photovoltaics **3**, 1271–1278 (2013).

[32]A. Khalili, A. Tibaldi, F. Elsehrawy, and F. Cappelluti, "Multiscale device simulation of quantum dot solar cells," Proceedings of SPIE **10913**, 59 (2019).

[33]M. O. Watanabe, J. Yoshida, M. Mashita, T. Nakanisi, and A. Hojo, "Band discontinuity for GaAs/AlGaAs heterojunction determined by C-V profiling technique," Journal of Applied Physics **57**, 5340–5344 (1985).

[34]B. F. Levine, "Quantum-well infrared photodetectors," Journal of Applied Physics **74** (1993), 10.1063/1.354252.

[35]D. Colombo, S. Sanguinetti, E. Grilli, M. Guzzi, L. Martinelli, M. Gurioli, P. Frigeri, G. Trevisi, and S. Franchi, "Efficient room temperature carrier trapping in quantum dots by tailoring the wetting layer," Journal of Applied Physics **94**, 6513–6517 (2003).

[36]J. A. Venables, "Nucleation calculations in a pair-binding model," Physical Review B **36**, 4153–4162 (1987).

[37]S. Bietti, C. Somaschini, N. Koguchi, C. Frigeri, and S. Sanguinetti, "Self-Assembled Local Artificial Substrates of GaAs on Si Substrate," Nanoscale Research Letters **5**, 1905–1907 (2010).

[38]J. A. Sobrino and J. C. Jiménez-Muñoz, "Minimum configuration of thermal infrared bands for land surface temperature and emissivity estimation in the context of potential future missions," Remote Sensing of Environment **148**, 158–167 (2014).